Bioorganic & Medicinal Chemistry Letters 21 (2011) 4773–4778

Contents lists available at ScienceDirect

Bioorganic & Medicinal Chemistry Letters

journal homepage: www.elsevier.com/locate/bmcl

Identification of 2-oxatriazines as highly potent pan-PI3K/mTOR dual inhibitors

Christoph M. Dehnhardt [a,*], Aranapakam M. Venkatesan [a], Zecheng Chen [a], Efren Delos-Santos [a], Semiramis Ayral-Kaloustian [a], Natasja Brooijmans [b], Ker Yu [c], Irwin Hollander [c], Larry Feldberg [c], Judy Lucas [c], Robert Mallon [c]

[a] Medicinal Chemistry, Pfizer, 401 N. Middletown Rd., Pearl River, NY 10965, USA
[b] Computational Chemistry, Pfizer, 401 N. Middletown Rd., Pearl River, NY 10965, USA
[c] Oncology, Pfizer, 401 N. Middletown Rd., Pearl River, NY 10965, USA

ARTICLE INFO

Article history:
Received 20 April 2011
Revised 12 June 2011
Accepted 14 June 2011
Available online 21 June 2011

Keywords:
Oxatriazine scaffold
PI3K
mTOR
Akt
PKI-587
PKI-402

ABSTRACT

We recently described several highly potent, triazine (**1**) and triazolopyrimidine (**2**) scaffold-based, dual PI3K/mTOR-inhibitors (e.g., **1**, PKI-587) that were efficacious in both in vitro and in vivo models. In order to further optimize these compounds we devised a novel series, the 2-oxatriazines, which also exhibited excellent potency and good metabolic stability. Some 2-oxatriazines showed promising in vivo biomarker suppression and induced apoptosis in the MDA-MB-361 breast cancer xenograft model.

Class I phosphatidylinositol 3-kinases (PI3Ks) play a key role in the biology of human cancer.[1] PI3Ks are divided into three classes (I–III) based on their structures, mode of regulation, and substrate preference.[1] Class IA PI3Ks are comprised of three isoforms (p110α, p110β and p110δ) that have a common regulatory subunit (p85), and are primarily activated by signals from receptor tyrosine kinases (RTKs). The class IB PI3K (p110γ) is structurally similar, but it has a different regulatory subunit (p101), and it is exclusively activated by G-protein coupled receptors.

PI3Ks phosphorylate the 3′-OH position of the inositol ring of the membrane phospholipid, phosphatidylinositol-bisphosphate(4,5) (PIP2), to form the phosphatidylinositol-triphosphate(4,5,6) PIP3. PIP3 recruits pleckstrin homology domain containing proteins, such as PDK1 and Akt, to the inner cell surface where PDK1 phosphorylates and actiavtes Akt,[1] which in turn leads to mTOR activation. mTOR, a PI3K related kinase (PIKK) family member, is a component of the mTORC1 and mTORC2 serine/threonine kinase complexes, which play key roles in cell homeostasis and growth, and are abnormally regulated in tumor cells.

Aberrant activation of the PI3K signaling cascade stimulates cell growth, survival, proliferation, and migration. These events not only promote the formation of malignant tumors, but also enhance the development of inflammatory and autoimmune diseases. More than 50% of all solid tumors have gene mutations, deletions, or amplifications that lead to upregulated PI3K/Akt/mTOR signaling.[1] Therefore, blocking the PI3K/Akt/mTOR signaling pathway by inhibiting both PI3K lipid and mTOR serine/threonine kinase activity provides an innovative strategy for cancer therapy. Dual PI3K/mTOR inhibitors such as PKI-402[5] and PKI-587[4] inhibit all p110 isoforms, as well as mTORC1 and mTORC2.[2] These molecules effectively block PI3K/Akt/mTOR signaling in cancers with mutations in PIK3CA and PIK3R1, PTEN loss, and RTK-dependent activation.[2] Dual PI3K/mTOR inhibitors also mitigate the feedback activation of PI3K signaling caused by selective mTORC1 inhibitors (i.e., rapamycin and its analogs), and because of this they may yield greater therapeutic benefit in cancer patients.[2] The strong antiproliferative activities of dual PI3K/mTOR inhibitors have already been demonstrated by the highly efficacious compounds, PKI-402 and PKI-587, shown in Figure 1, and others.[3] Here we describe a novel series, the 2-oxatriazines, which exhibited similar potency to PKI-402 and PKI-587 and good metabolic stability.

Compounds **1**[4] and **2**[5] are recently reported dual pan-PI3K/mTOR inhibitors that utilize the morpholine oxygen for the key hinge region hydrogen bonding interaction in the ATP pocket of both class I PI3Ks and mTOR. Analog **1** is a bismorpholinotriazine, and since only one morpholino group is needed for binding to the PI3K hinge region, the second morpholine of **1** can be replaced with other groups to further optimize compound properties and biological

* Corresponding author.
E-mail addresses: christoph.dehnhardt@pfizer.com, christophd@me.com (C.M. Dehnhardt).

0960-894X/$ - see front matter © 2011 Elsevier Ltd. All rights reserved.
doi:10.1016/j.bmcl.2011.06.063

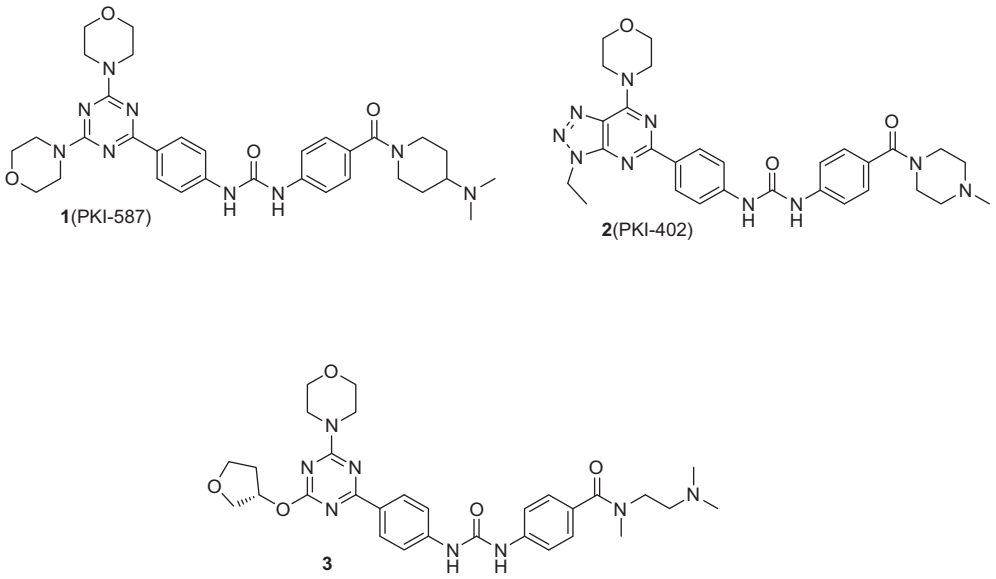

Figure 1. **1**(PKI-587) and **2**(PKI-402) are recently reported dual PI3K/mTOR inhibitors. Compound **3** is a novel dual pan-PI3K/mTOR inhibitor which has an efficacy profile comparable to that of **1** and **2**.

profiles. Many triazine inhibitors have been disclosed in the recent literature,[6] while 2-oxatriazine-based PI3K inhibitors provided novelty due to their rare use as kinase-inhibitors. Thus, we synthesized[7] 2-oxatriazines to generate a back-up series for **1**. First, we wanted to enhance the potency of this scaffold utilizing previously known SAR information, such as the introduction of benzamido ureas. This effort culminated in the discovery of **3**, a compound which showed an in vitro and in vivo potency profile similar to that of **2**, particularly in regard to in vivo biomarker suppression. In this publication we describe the SAR studies leading to **3**.

The synthesis of oxatriazines **8**–**24** is shown in Scheme 1. Cyanuric chloride **4** was aminated with morpholine at 0 °C to give the 1,3-dichloro-5-morpholino triazine **5**, which was reacted with the appropriate lithiumalkanolate to give **6a**–**e**.

Subsequently, **6a**–**e** were converted to anilines **7a**–**e** by reaction with 4-aminophenylboronic acid pinacolester under Suzuki conditions. Compounds **7a**–**e** were condensed with the appropriate 4-aminobenzamide analogues **9a**–**d** under triphosgene activation to obtain ureidobenzamides **3**, **8**–**24**. For SAR purposes, we were also interested in keto tautomers of 2-oxatriazines, such as **27**. The synthesis of **27** is shown in Scheme 2. Dichlorotriazine **5** was treated with 1 N NaOH at room temperature to give **25**, which was coupled with **26** under Suzuki conditions to give **27**. The structure of **27** was determined by 2D NMR indicating that **28** is the major tautomer in DMSO solution.

All final compounds were tested for inhibition[5] of PI3Kα, PI3Kγ, and mTOR kinase activity. Due to the compelling efficacy profile of **1**[4,8,9] and the fact that compounds **1** and **2** show no oral bioavailability, we were interested in an iv administered compound. Hence, we limited our pharmaceutical profiling to relevant data such as solubility at pH 7.4, and to stability studies in rat, nude mouse, and human liver microsomes to mimic hepatic clearance. The physical properties and biological data for analogues **3**, **8**–**24** and **27** are shown in Table 1.

Initially the effect of a small substituent such as the methoxy group (**8**–**13**) at the 2-position of the triazine core was evaluated. These analogues showed good potency (IC_{50} <3 nM) against PI3Kα, with moderate selectivity over PI3Kγ and mTOR. In fact, some methoxy substituted compounds (**9**–**13**) showed between 9- and 29-fold selectivity between PI3Kα and mTOR. Furthermore, derivatives **8**–**13** exhibited good aqueous solubility at pH 7.4. In addition, compounds **8**–**13** showed good microsomal stability in various species, except for **9** and **12** which showed only moderate stability in rat microsomes. Tumor cell growth inhibition by the methoxy analogues **8**–**13** was not as potent as that found for compounds **1** or **2**. Analogue **9**, the best compound in this subset, still showed a more than twofold lower potency against MDA-MB-361 and PC3-cells compared to compound **1**.

Replacing the methoxy group with an isopropoxy group led to compounds **15**–**18**, which in general exhibited good potency against PI3Kα and mTOR, but lower selectivity for PI3Kα/mTOR relative to methoxy analogues **8**–**13**. For example, compound **17** exhibited no selectivity for PI3Kα/mTOR, while compound **9** showed 19-fold selectivity. Compound **9** also showed better PI3Kα potency than **17**. However, compound **17** showed better tumor cell growth inhibition then **9**. Analogue **17** was overall the most potent *i*-PrO substituted derivative in enzyme and tumor growth inhibition, and showed moderate solubility at physiological pH as well as good stability against rat, nude mouse, and human microsomes. Introducing the more bulky O-tropinyl group in **24** led to good enzyme potency against PI3Kα and mTOR but low cell potency. It is not clear if this result has to do with the physical properties such as the high tPSA (=146) of **24**. However, in other series[10,11] we also observed relatively low cell potency for compounds carrying a basic nitrogen in a similar region of the molecule.

The unsubstituted oxatriazine **27** showed moderate potency against PI3Kα, strong selectivity for PI3Kα/mTOR (>100-fold), and weak cell potency. Following 2D NMR studies we could show that **27** predominantly exist as triazine-one tautomer carrying the H at N-5. The steric clash of the 5-H with the morpholine 3-CH_2 could lead to a slight rotation of the morpholine out of plane which could lower its ability to bind to Val851 in the hinge region, resulting in lower potency against PI3Kα. The mTOR selectivity may be explained by a similar phenomenon with regard to the 6-aryl-appendage. Here, the 5-H could lead to a slight rotation around the aryl group. Rotation around the C-2 aryl C–C bond has already been reported to give a rise in selectivity for PI3Kα over mTOR series. For example, Sutherlin et al.[12] showed that 2-methyl-5aminopyrimidines show 100-fold selectivity of PI3Kα/mTOR compared the non methyl-substituted analog. In their case this observation was rationalized based on X-ray co-crystal with PI3Kγ and docking in a mTOR homology models showing that the methyl group

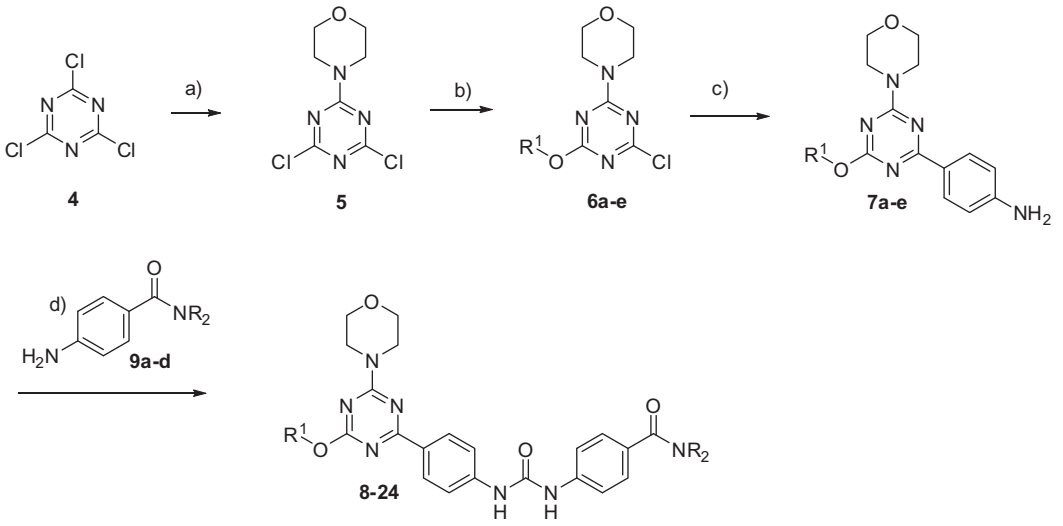

a) NEt_3, morpholine, 0 °C, 92%, b) R^1OH, BuLi, THF c) $(Ph_3P)_4Pd$, 4-aminophenylboronic acid pinacol ester, Na_2CO_3, DME, 140 °C,1h, μW; d) triphosgene, NEt_3, **9a-d**.

8, R^1 = OMe, NR_2 = -NH-$(CH_2)_2$-1-piperidine
9, R^1 = OMe, NR_2 = -NMe-$(CH_2)_2$-NMe_2
10,R^1 = OMe, NR_2 = -NH-$(CH_2)_2$-NMe_2
11, R^1= OMe, NR_2 = -NMe-$(CH_2)_2$-NHMe
12, R^1= OMe, NR_2 = 4-methylpiperazine
13, R^1 = OMe, NR_2 = 3,3-dimethylpiperazine
14, R^1 = 3-oxetanyloxy, NR_2 = 4-methylpiperazine
15, R^1 = O*i*-Pr, NR_2 = 4-methylpiperazine
16, R^1 = O*i*-Pr, NR_2 = 4-NH-1-methylpiperidine
17, R^1 = O*i*-Pr, NR_2 = -NMe-$(CH_2)_2$-NMe_2
18, R^1 = O*i*-Pr, NR_2 = -NH-$(CH_2)_2$-NMe_2
3, R^1 = O-3-(S)-tetrahydrofuranyl, NR_2 = -NMe-$(CH_2)_2$-NMe_2
19, R^1 = O-3-(S)-tetrahydrofuranyl, NR_2 = 4-Me_2N-piperidine
20, R^1 = O-3-(S)-tetrahydrofuranyl, NR_2 = -NH-$(CH_2)_2$-1-piperidine
21, R^1 = O-3-(S)-tetrahydrofuranyl, NR_2 = -NH-$(CH_2)_2$-1-pyrrolidine
22, R^1= O-3-(S)-tetrahydrofuranyl, NR_2 = 4-methylpiperazine
23, R^1 = O-3-(S)-tetrahydrofuranyl, NR_2 = 4-Me_2N-piperidine
24, R^1 = O-tropinyl, NR_2 = NH_2

Scheme 1. General synthetic route to 2-oxatriazines **3**, **8**–**24**.

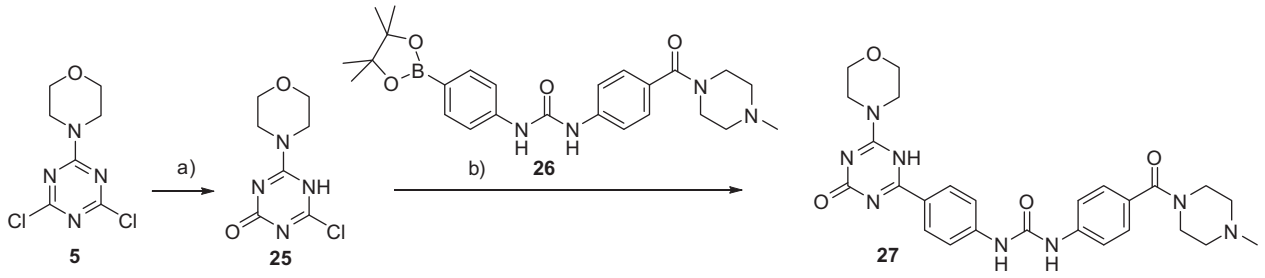

a) 1N NaOH/THF (1:1), rt (64%); b) Na_2CO_3, DME, 140 °C, 1h μW (23%).

Scheme 2.

twisted the the aryl group out of plane due to a steric clash of the methyl group with Tyr867 in mTOR. Now, the methyl is oriented toward a region where residue differences between PI3K and mTOR exist. A similar phenomen could play a role for compound **24** just that here it is a steric clash between H–N and CH.

Introduction, of a 3-oxyoxetanyl group in 2-position led to compound **14**. Analogue **14** and the *i*-Pr analogue **15** exhibited very similar profiles in cell proliferation assays. However, **14** showed better potency against PI3Kα, and lower potency against mTOR, relative to **15**. The introduction of hydrogen bond acceptors such as the O in the oxetane led to increased potency against PI3Kα. In addition, other compounds such as **1** carrying an O-containing morpholine, where the oxygen roughly occupies the same region, also showed excellent potency against PI3Kα.[4] However, to our best knowledge this effect is not caused by an interaction with amino acid residues in the ATP- binding pocket of PI3Kα. Hence, we decided to use ligand based design to look for groups that mimic the molecular shape of the 2-position morpholine group of **1** as the second triazine substituent. Several analogues with 2-substituents were modeled and overlayed with compound **1**. In this study, the 2-(*S*)-oxytetrathydofuryl group of **3** showed an almost perfect overlap with the second morpholine in **1**. Figure 2 shows an overlay of **1** and **3** docked in a PI3Kα homology model. As modeling suggests, the morpholine and 3-oxy-THF group occupy the same space, thus allowing identical binding of the morpholine oxygen to Val851, the urea O with Lys802, and the NH with Asp810, which

Table 1
Biological data and physical properties for 2-oxatriazine analogues **3**, **8**–**24**, and **27**

Compound	IC_{50}[a] (nM)					Solubility[b] @pH 7.4	$t_{1/2}$[c] (min)		
	PI3Kα	PI3Kγ	mTOR	MDA-361[d]	PC3[e]		Human	N. Mouse	Rat
8	2.0	20.5	8.2	<31	69	>100	>30	>30	>30
9	0.4	7.0	7.7	15	34	>100	>30	>30	15
10	0.6	10.5	5.6	<31	71	>100	>30	>30	>30
11	0.8	9.5	14.5	110	374	>100	>30	>30	>30
12	1.2	13.5	22.5	35	91	3	>30	>30	16
13	1.4	4.0	18.5	30	111	61	>30	>30	29
14	0.6	9.5	3.0	4	32	4	ND	ND	>30
15	3.0	49.5	1.3	5	33	0	>30	>30	17
16	1.4	22.0	1.3	<30	52	4	>30	>30	19
17	1.0	18.0	0.3	5	13	15	>30	23	>30
18	3.0	24.5	0.4	11	41	3	>30	>30	>30
3	0.2	4.8	0.7	3	9	>100	>30	>30	27
19	1.0	6.5	1.1	4	24	>100	18	>30	>30
20	1.4	8.0	0.4	5	18	1	>30	>30	27
21	1.4	6.0	0.3	8	27	23	>30	>30	28
22	1.7	14.3	1.7	6	21	1	15	>30	20
23	1.4	7.2	1.2	4	11	10	29	>30	16
24	3.2	72.5	5.3	2917	4453	62	ND	ND	4
27	15	96.5	1200	>1000	>1000	ND	ND	ND	>30
1	0.4	11	0.4	3	11	15	>30	>30	>30
2	1	9	2	8	21	0	>30	>30	15

[a] The values are an average of at least two separate determinations with a typical variation of less than ±30%.
[b] [μg/mL].
[c] Half-life of drug when incubated for 30 min with liver microsomes of the species shown.
[d] Breast cancer cell line.
[e] Prostate cancer cell line.

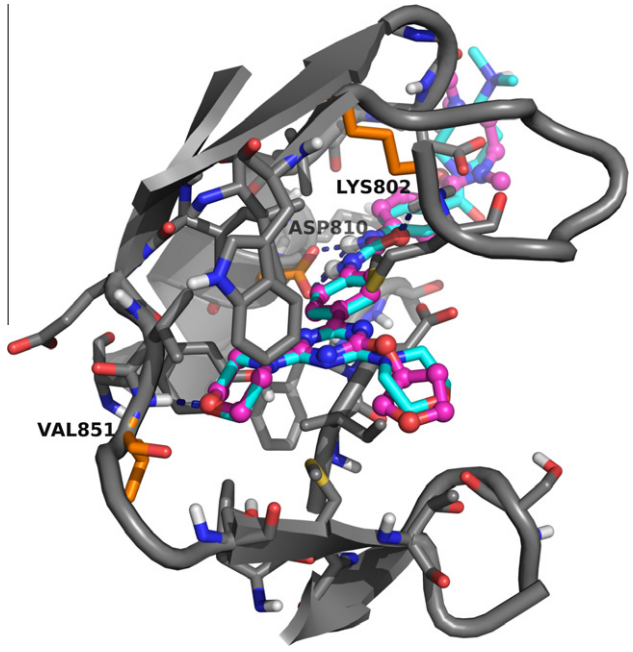

Figure 2. Overlay of compound **1** (cyan carbons, stick representation) and **3** (magenta carbons, ball-and-stick representation) docked in a PI3Kα homology model. Residues that form critical hydrogen bonding interactions are shown with orange carbons such as binding of morpholine to the hinge region Val851 and the urea oxygen to Lys802 and urea hydrogen to Asp810.

is consistent with their very similar enzyme potencies. Based on this modeling[13] we designed and synthesized novel analogues, where binding features to the hinge region as well as the aryl ureido-group interactions remained unchanged.

Indeed, compounds **3**, **19**–**23** showed good potency against PI3Kα and excellent potency in tumor cell growth inhibition assays. Among these analogues, **3** showed the best in vitro potency profile (IC_{50} values: PI3Kα, enzyme, 0.2 nM; MDA-MB-361 and PC3 tumor cell lines, 3 and 9 nM, respectively), paired with high solubility and good stability in rat, nude, mouse, and human microsomes. Hence, compound **3** was chosen for an in vivo side by side comparison with our clinical candidate **1**.

Compounds **1** and **3** were administered at 10 and 25 mg/kg in mice bearing MDA-MB-361 xenografts. Figure 3 shows that both compounds **1** and **3**, given at 25 mg/kg (iv), suppressed phosphorylated p-Akt-T308, p-Akt-S473, p-p70S6K, and p-S6 (p-Akt-S473, p-p70S6K, and p-S6 are mTOR specific biomarkers[5] and p-Akt-T308 is consistent with their in vitro profiles. Both **1** and **3** not only suppressed these PI3K/mTOR biomarkers for at least 8 h, but they also induced cleaved poly-adenosine-diphosphate-ribose polymerase (cPARP), a marker for cells undergoing apoptosis.[14] However, this study showed that **3** had a somewhat less profound biological effect on PI3K and mTOR specific biomarkers than our clinical candidate **1**. In fact, compound **3** administered at 25 mg/kg, achieved similar biomarker suppression to that observed with analog **1** given at 10 mg/kg. Furthermore, compound **3** displayed a much stronger biomarker response than previously reported for our first preclinical candidate **2**.[9] For example, compound **3** showed 8 h activation of cPARP when 25 pmk were dosed, while **2** showed cPARP induction only at higher dose (50 mpk). Clearly further investigation of **3** needs to be conducted to discover the full potential of this compound.

In summary, we introduced a novel 2-oxatriazine scaffold that was optimized using ligand based design and modeling. Novel analogues based on this 2-oxatriazine scaffold showed good potency against PI3Kα and mTOR, and good potency in tumor cell (MDA-MB-361[breast], PC3 [prostate]) growth inhibition assays. Compound **3** showed an in vitro profile superior to that of preclinical candidate **2** and comparable to clinical candidate **1**. Furthermore, in vivo biomarker studies showed that compound **3** was more potent than compound **2**, but not quite as potent as **1**. More result from our ongoing optimization effort of **3** will be reported in due course.

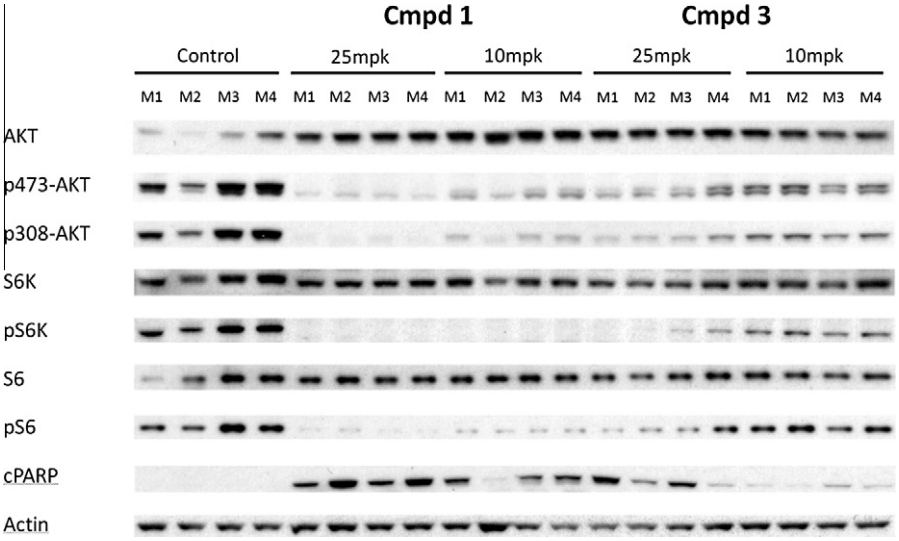

Figure 3. In vivo biomarker analysis at 8 h after compounds **1** and **3** were administered at 10 and 25 mg/kg (iv) to MDA-MB-361 tumor bearing nude mice.

Acknowledgments

The authors thank Dr. Joseph Ashcroft for advanced 2D NMR experiments and the Pearl River Chemical Technologies group for their support.

References and notes

1. Liu, P.; Cheng, H.; Roberts, T. M.; Zhao, J. J. *Nat. Rev.* **2009**, *8*, 627.
2. Engelman, J. A. *Nat. Rev. Cancer* **2009**, *9*, 550.
3. (a) Stauffer, F.; Maira, S. M.; Furet, P. *Bioorg. Med. Chem. Lett.* **2008**, *18*, 1030; (b) Maira, S. M.; Stauffer, F.; Brueggen, J.; Furet, P.; Schnell, C.; Fritsch, C.; Brachmann, S.; Chene, P.; De Pover, A.; Schemaker, K.; Fabbro, D.; Gabriel, D.; Simonen, M.; Murphy, L.; Finan, P.; Sellers, W.; Garcia-Echeverria, C. *Mol. Cancer Ther.* **2008**, *7*, 1851; (c) Cheng, H.; Bagrodia, S.; Bailey, S.; Edwards, M.; Hoffman, J.; Hu, Q.; Kania, R.; Knighton, D.; Marx, M.; Ninkovic, S.; Sun, S.; Zhang, E. *Med. Chem. Commun.* **2010**, *1*, 139; (d) Knight, S. D.; Adams, N. D.; Burgess, J. L.; Chaudhari, A. M.; Darcy, M. G.; Donatelli, C. A.; Luengo, J. I.; Newlander, K. A.; Parrish, C. A.; Ridgers, L. H.; Sarpong, M. A.; Schmidt, S. J.; Van Aller, G. S.; Carson, J. D.; Diamond, M. A.; Elkins, P. A.; Gardiner, C. M.; Garver, E.; Gilbert, S. A.; Gontarek, R. R.; Jackson, J. R.; Kershner, K. L.; Luo, L.; Raha, K.; Sherk, C. S.; Sung, C.-M.; Sutton, D.; Tummino, P. J.; Wegrzyn, R. J.; Auger, K. R.; Dhanak *Med. Chem. Lett.* **2010**, *1*, 39; (e) Chen, Z.; Venkatesan, A. M.; Dehnhardt, C. M.; Ayral-Kaloustian, S.; Brooijmans, N.; Mallon, R.; Feldberg, L.; Hollander, I.; Lucas, J.; Yu, K.; Kong, F.; Mansour, T. S. *J. Med. Chem.* **2010**, *53*, 3169; (f) D'Angelo, N. D.; Kim, T.-S.; Andrews, K.; Booker, S. K.; Caenepeel, S.; Chen, K.; Freeman, D.; Jiang, J.; McCarter, J. D.; San Miguel, T.; Mullady, E. L.; Schrag, M.; Subramanian, R.; Tang, J.; Wahl, R. C.; Wang, L.; Whittington, D. A.; Wu, T.; Xi, N.; Xu, Y.; Yakowec, P.; Zalameda, L. P.; Zhang, N.; Hughes, P.; Norman, M. H. *J. Med. Chem.* **2011**, *54*, 1789; (g) Burger, M. T.; Knapp, M.; Wagman, A.; Ni, Z.-J.; Hendrickson, T.; Atallah, G.; Zhang, Y.; Frazier, K.; Verhagen, J.; Pfister, K.; Ng, S.; Smith, A.; Bartulis, S.; Merrit, H.; Weismann, M.; Xin, X.; Haznedar, J.; Voliva, C. F.; Iwanowicz, E.; Pecchi, S. *ACS Med. Chem. Lett.* **2011**, *2*, 34.
4. Venkatesan, A. M.; Dehnhardt, C. M.; Delos Santos, E.; Dos Santos, O.; Ayral-Kaloustian, S.; Khafizova, G.; Brooijmans, N.; Mallon, R.; Hollander, I.; Feldberg, L.; Lucas, J.; Yu, K.; Gibbons, J.; Abraham, R. T.; Chaudhary, I.; Mansour, T. S. *J. Med. Chem.* **2010**, *53*, 2636.
5. Dehnhardt, C. M.; Venkatesan, A. M.; Delos Santos, E.; Chen, Z.; Santos, O.; Ayral-Kaloustian, S.; Brooijmans, N.; Mallon, R.; Hollander, I.; Feldberg, L.; Lucas, J.; Chaudhary, I.; Yu, K.; Gibbons, J.; Abraham, R.; Mansour, T. S. *J. Med. Chem.* **2010**, *53*, 798.
6. Venkatesan, A. M.; Chen, Z.; Dos Santos, O.; Dehnhardt, C.; Santos, E. D.; Ayral-Kaloustian, S.; Mallon, R.; Hollander, I.; Feldberg, L.; Lucas, J.; Yu, K.; Chaudhary, I.; Mansour, T. S. *Bioorg Med. Chem. Lett.* **2010**, *20*, 5869.
7. Synthesis of (*S*)-*N*-(2-(dimethylamino)ethyl)-*N*-methyl-4-(3-(4-(4-morpholino-6-((tetrahydrofuran-3-yl)oxy)-1,3,5-triazin-2-yl)phenyl)ureido)benzamide **3**: A solution of (*S*)-tetrahydrofuran-3-ol (1.874 g, 21.27 mmol) in THF (32 mL) was cooled to −78 °C and n-butyl lithium in hexanes (11.06 ml, 27.7 mmol) was slowly added. The mixture was stirred for 0.5 h and a solution of **5** 4-(4,6-dichloro-1,3,5-triazin-2-yl)morpholine (5 g, 21.27 mmol) in THF (16 mL) was added. Stirring was continued for 2 h at −78 °C and the mixture was allowed to warm to 22 °C overnight. The reaction was quenched with sat. NH_4Cl solution and extracted with ether (3 × 20 mL). The combined fractions were dried over $MgSO_4$. After filtration of $MgSO_4$, the mixture was concentrated and purified by flash chromatography using Isco-combiflash eluting with EtOAc:Hex (1:1). The combined product fractions were distilled to dryness to give 2.8 g (46%) of the product as a white solid.
^{1}H NMR ($CDCl_3$) δ 5.51 (m, 1H), 4.06 (m, 1H), 4.00–3.81 (m, 7H), 3.73 (m, 4H), 2.19 (m, 2H) ppm. MS (ESI) *m*/*z* 287.1.
To a microwave vial was added **6d** (*S*)-4-(4-chloro-6-(tetrahydrofuran-3-yloxy)-1,3,5-triazin-2-yl)morpholine (1 g, 3.49 mmol), 4-(4,4,5,5-tetramethyl-1,3,2-dioxaborolan-2-yl)aniline (1.146 g, 5.23 mmol), Na_2CO_3 aq 2 M (3.49 ml, 6.98 mmol), $Pd(Ph_3P)_4$ (0.403 g, 0.349 mmol) and DME (10 ml) and the mixture was heated for 1 h to 140 °C in a microwave oven. After completion, the reaction mixture was filtered. The filtrate was evaporated and purified by flash chromatography using Isco-combiflash eluting with EtOAc:Hex (1:1). The combined product fractions were distilled to dryness to give 665 mg (of the product. as beige solid.
^{1}H NMR ($CDCl_3$) δ: 8.24 (d, *J* = 8.6 Hz, 2H), 6.90 (d, *J* = 8.6 Hz, 2H), 5.61 (m, 1H), 4.30 (m, 1H), 4.04–3.73 (m, 11H), 2.26 (m, 2H), 1.57 (m, 2H) ppm.
MS (ESI) *m*/*z* 344.2.
To a stirred solution of triphosgene (0.373 mg, 1.258 μmol) in anhydr. THF (20 ml) was added **7d** (*S*)-4-(4-morpholino-6-(tetrahydrofuran-3-yloxy)-1,3,5-triazin-2-yl)aniline (1.200 mg, 2.097 μmol) at 25 °C. The reaction mixture was stirred for 5 min and NEt_3 (45 mL, 0.33 mmol) were added and the reaction mixture was stirred for additional 1 h. Then **9a** 4-amino-*N*-(2-(dimethylamino)ethyl)-*N*-methylbenzamide (1.392 mg, 6.29 μmol) was added and stirred for another 0.5 h and NEt_3 (406 mL, 2.91 mmol) was added and the mixture was stirred over night. The solvents were removed in a N_2 stream and the crude mixture was purified by semi-prep-HPLC to obtain **3** as an off white solid (665 mg, 53%). ^{1}H NMR (DMSO) δ: 9.11 (s, 1H), 8.97 (s, 1H), 8.29 (d, *J* = 8.9 Hz, 2H), 7.59 (d, *J* = 8.9 Hz, 2H), 7.51 (d, *J* = 8.6 Hz, 2H), 7.33 (d, *J* = 8.6 Hz, 2H), 5.59 (m, 1H), 4.00–3.68 (m, 12H), 3.40 (m, 2H), 2.95 (s, 3H0, 2.40 9 m, 2H), 2.30–2.07 (m, 8H) ppm.
MS (ESI) *m*/*z* 591.3 Analytical LC using Prodigy ODS3 column, ACN/H_2O eluent at 1 mL/min flow (containing 0.05% TFA), 20 min. gradient 5% ACN to 95% ACN, monitored by UV absorption at 215 nm showed 99.4% purity.
8. Mallon, R. G.; Feldberg, L. R.; Lucas, J.; Chaudhary, I.; Dehnhardt, C.; Delos Santos, E.; Chen, Z.; dos Santos, O.; Ayral-Kaloustian, S.; Venkatesan, A.; Hollander, I. *Clin. Cancer Res.* **2011**, *17*, 3193.
9. Mallon, R.; Hollander, I.; Feldberg, L. L.; Lucas, J.; Gibbons, J.; Venkatesan, A. M.; Dehnhardt, C. M.; Delos Santos, E.; Chen, Z.; dos Santos, O.; Ayral-Kaloustian, S.; Brooijmanns, S.; Soloveva, V. *Mol. Cancer Ther.* **2010**, *9*, 976.
10. Dehnhardt, C. M.; Venkatesan, A. M.; Chen, Z.; Delos Santos, E.; Santos, O.; Bursavich, M.; Brooijmans, B.; Mallon, R.; Hollander, I.; Feldberg, L. Lucas, J.; Yu, K. Ayral-Kaloustian, S.; Gibbons, J.; Abraham, R.; Mansour T. S. Novel Imidazolopyrimidines as Dual PI3-Kinase/mTor Inhibitors Proceedings of the 100th Annual Meeting of the American Association for Cancer Research; 2009 Apr 18–22; Denver, CO; AACR; 2009; Abstract nr 2017.
11. Venkatesan, A. M.; Dehnhardt, C. M.; Chen, Z.; Delos Santos, E.; Dos Santos, O.; Bursavich, M.; Gilbert, A. M.; Ellingboe, J. W.; Ayral-Kaloustian, S.; Khafizova, G.; Brooijmans, N.; Mallon, R.; Hollander, I.; Feldberg, L.; Lucas, J.; Yu, K.; Gibbons, J.; Abraham, R.; Mansour, T. S. *Bioorg. Med. Chem. Lett.* **2010**, *20*, 653.
12. Sutherlin, D. P.; Sampath, D.; Berry, M.; Castanedo, G.; Chang, Z.; Chuckowree, I.; Dotson, J.; Folkes, A.; Friedman, L.; Goldsmith, R.; Heffron, T.; Lee, L.; Lesnick, J.; Lewis, C.; Mathieu, S.; Nonomiya, J.; Olivero, A.; Pang, J.; Prior, W. W.;

Salphati, L.; Sideris, S.; Tian, Q.; Tsui, V.; Wan, N. C.; Wang, S.; Wiesmann, C.; Wong, S.; Zhu, B.-Y. *J. Med. Chem.* **2010**, *53*, 1086.
13. Zask, A.; Verheijen, J. C.; Curran, K.; Kaplan, J.; Richard, D. J.; Nowak, P.; Malwitz, D. J.; Brooijmans, N.; Bard, J.; Svenson, K.; Lucas, J.; Toral-Barza, L.; Zhang, W.; Hollander, I.; gibbons, J. J.; Abraham, R. T.; Ayral-Kaloustian, S.; Mansour, T. S.; Yu, K. *J. Med. Chem.* **2009**, *52*, 5013.
14. Golas, J. M.; Arndt, K.; Etienne, C.; Lucas, J.; Nardin, D.; Gibbons, J.; Frost, P.; Ye, F.; Boschelli, D. H.; Boschelli, F. *Cancer Res.* **2003**, *63*, 375.